Biosystems Engineering (2005) **92** (1), 119–133
doi:10.1016/j.biosystemseng.2005.06.008
SW—Soil and Water

Correlation between Ground Measured Soil Moisture and RADARSAT-1 derived Backscattering Coefficient over an Agricultural Catchment of Navarre (North of Spain)

Jesús Álvarez-Mozos[1]; Javier Casalí[1]; María González-Audícana[1]; Niko E.C. Verhoest[2]

[1]Department of Projects and Rural Engineering, Public University of Navarre, Arrosadia, 31006 Pamplona, Spain; e-mail of corresponding author: jesus.alvarez@unavarra.es
[2]Laboratory of Hydrology and Water Management, Coupure links 653, 9000 Ghent, Belgium; e-mail: niko.verhoest@ugent.be

(Received 11 October 2004; accepted in revised form 22 June 2005; published online 15 August 2005)

Surface soil moisture is a variable of great importance in several agronomic, hydrological and meteorological processes. The knowledge of its magnitude and its spatial distribution is essential to adequately describe and model the processes where it is involved.

Radar remote sensors measure microwave energy backscattered by natural surfaces. This scattered energy depends on the geometrical and the dielectric properties of surfaces. In the case of bare soil surfaces, the dielectric properties are directly related to the soil water content, so theoretically, radar remote sensing allows the extraction of spatially distributed soil moisture information. However, the influence of surface roughness on the scattering process limits the ability to correctly estimate volumetric soil moisture values unless detailed roughness measurements are acquired.

The present paper reports the results of a study where five images from the remote radar sensor on the satellite RADARSAT-1 were processed and correlated to ground measured soil moisture values over an agricultural catchment. Linear regression models were fitted between RADARSAT-1 derived backscattering coefficient σ^0 and the soil moisture at different spatial scales: point scale, field scale and catchment scale.

Three soil moisture classes were identified according to their implications for crop growth: (1) low moisture values which contributed to water stress in plants; (2) medium moisture content that allowed an optimal crop growth; and (3) high moisture values which affected crop growth by other means, such as by fungal disease.

Results show a direct relation between σ^0 and the soil moisture. At the catchment scale the observed correlation is high. At detailed scales, however, variability increases, causing a decrease of correlation values. The ability of σ^0 to discriminate between the considered moisture classes seems to be adequate. The accuracy of the estimation increases from the detailed to coarser scales.

In the case of vegetated fields, the vegetation cover can cause a certain attenuation of the radar pulse resulting in reduced σ^0 values. In this research, vegetation-induced attenuation was considered by applying the semi-empirical 'Water Cloud' model.

The presented technique is useful for crop growth monitoring and modelling at medium to large scales, particularly in early growing seasons where the attenuation of vegetation is not too high. It is also applicable to irrigation planning or crop health studies. However, regression lines are site specific and can be affected by the surface roughness variability and vegetation cover of fields.

1. Introduction

Surface soil moisture is a variable that plays a crucial role in various processes occurring on the soil–atmosphere interface. At high spatial scales, it influences meteorological and climatic processes (Burman, 2003; Chanzy, 2003). At medium scales, it determines hydrological and agronomic processes such as runoff generation (Jackson, 1980; O'Loughlin, 1986; Georgakakos & Baumer, 1996; Kirkby, 2001), and evapotranspiration, crop development or irrigation needs (Wetzel & Chang, 1987; Quesney *et al*., 2000; Troch *et al*., 2003). Surface soil moisture also influences soil erosion processes such as gully and rill erosion and headcut appearance (Montgomery & Dietrich, 1988; Moore *et al*., 1988; Casalí *et al*., 1999; Kirkby, 2001; Romkens *et al*., 2001) or landslide occurrence. At small scales, it exerts a high influence on biogeochemical processes such as pollutant migration and, as a result, it is related to water quality issues (Famiglietti *et al*., 1999; Huisman *et al*., 2002).

Surface soil moisture characterisation is a complicated task due to its high spatial and temporal variability (Kachanoski *et al*., 1988). Soil moisture variations normally follow rainfall trends. Four factors are significant when determining the variations in the moisture content of a soil: soil type; vegetation cover; tillage conditions or soil surface state; and topography. However, the evolution of the moisture content of soils is more difficult to predict, due to interactions between these factors.

In the field of hydrology, the soil moisture balance at a site is known to be the keystone of many fundamental processes because of its importance on crucial processes in the hydrologic cycle and its high variability (Rodríguez–Iturbe, 2000). Moreover, the application of hydrological simulation models and the accuracy of their predictions are strongly dependent on the knowledge of the water content of soils being simulated (Rowntree & Bolton, 1983; Troch *et al*., 1993; Cognard *et al*., 1995; Yu *et al*., 2001).

On the other hand, soil moisture monitoring is of great interest for agronomists. Low soil moisture values cause yield reductions. Furthermore, some growing stages are particularly sensitive to a lack of moisture. High soil moisture conditions also severely affect crop growth as the occurrence of fungal diseases and other pests is usually favoured to saturated areas.

Most of the soil moisture measuring methods which have become established consist of point-based probes which require the application of complex geostatistical techniques to obtain estimates over fields or larger areas (Kachanoski *et al*., 1988). In addition, the high spatial and temporal variability of the soil moisture makes it difficult to extrapolate from point-based measurements to larger scales.

Remote sensing provides a means of acquiring spatially distributed information of the land surface with a certain periodicity. The possibility of inferring the moisture content of soils from remote-sensing images has been intensively studied (Moran *et al*., 2004). Among the different types of remote sensors developed so far, radar sensors (*i.e.* ERS-1/2, RADARSAT-1, ENVISAT-ASAR) have the greatest potential for the estimation of soil moisture at the field or catchment scale (Moran *et al*., 2004).

Radar sensors are active microwave instruments that emit a radiation pulse towards a target (usually the Earth surface) and receive the echo, or backscattered pulse, that returns from the target. The principle of radar-based soil moisture estimation relies on the existing relation between the backscattering coefficient σ^0 in dB, defined as the ratio of the power of the returned pulse and that of the emitted pulse, and the dielectric properties of the observed soils, being the latter directly related to the moisture content of soils (Ulaby *et al*., 1982). Apart from that, the microwave radiation is not affected by cloud coverage and radar sensors can also operate during the night; these characteristics represent an additional benefit compared to optical sensors (*i.e.* LANDSAT, SPOT).

However, radar remote sensing also has its drawbacks. Over mountainous areas, radar images show distortions that strongly limit their interpretation. In addition, surface characteristics, such as roughness and vegetation cover, do have an influence on the backscattering coefficient, making it difficult to estimate the soil moisture unless very detailed knowledge of the roughness and vegetation cover is available (Altese *et al*., 1996). In fact, the ability of radar sensors to estimate the soil moisture can be completely hampered in the case of very dense and tall canopies such as forests. Crop canopies can also influence the backscattering coefficient; in order to minimise the influence of vegetation, radar images acquired at long wave bands and steep incident angles are preferred.

Several backscattering models have been proposed to relate the backscattering coefficient of a surface with its characteristics (soil moisture and surface roughness) (Ulaby *et al*., 1982, Oh *et al*., 1992; Fung, 1994). Models such as the 'Integral Equation Method' model (Fung, 1994), have shown a good performance over laboratory conditions (Mancini *et al*., 1999) but their application to natural conditions have yielded poor results (Altese *et al*., 1996). The main difficulty of their use over natural surfaces is related to the sensitivity of the models to the surface roughness parameters and the difficulty of correctly measuring those (Davidson *et al*., 2000). Therefore, the estimation of soil moisture from radar

images, based on those backscattering models, requires a very detailed knowledge of the surface roughness only achievable through intensive roughness measurement campaigns.

The main objective of the current research is to explore the feasibility of soil moisture estimation from radar remote sensors through a simplistic approach. The approach is based on the assumption of a linear relation between the backscattering coefficient of a surface and its soil moisture over homogeneous surface roughness conditions (Ulaby *et al.*, 1982). Surface roughness is assumed to depend only on the tillage practise performed and not to vary in time. Therefore, the approach does not require detailed roughness measurements, but only knowledge of the tillage operations performed on the fields.

A set of five RADARSAT-1 images was analysed and compared to ground-sampled soil moisture over an experimental catchment located in the region of Navarre (Northern Spain). The correlation between the backscattering coefficient and the soil moisture values is analysed at three different spatial scales: point scale, field scale and watershed scale. The spatial variability of surface roughness parameters is evaluated and its influence in the soil moisture estimation analysed. The influence of the existing cereal vegetation cover is also assessed through a semi-empirical 'Water Cloud' model (Attema & Ulaby, 1978). Finally, the possibility of identifying different soil moisture ranges is investigated at the field and catchment scale; and the practical implications and possible benefits for crop growth research and other related disciplines are discussed.

2. Materials and methodology

2.1. *Test site*

The present work was carried out over an agricultural watershed located in the mid-region of Navarre (North of Spain) called *La Tejería* (*Fig. 1*). This watershed forms part of the Experimental Agricultural Watershed Network of Navarre, created by the local Government of Navarre in 1993, to enable the impact of agriculture on hydrological resources to be studied (Donézar & del Valle de Lersundi, 2001).

After a detailed soil study (Government of Navarre, 2000), ten soil types were identified in the watershed. The most common soil type was classified as Tipic Xerorthent and covers most of the hillsides, forming relatively shallow soils (less than 1 m deep) with clayey textures. On the lower parts of the hillsides, the soils were found to be deeper (1·0–1·5 m), and the soil types

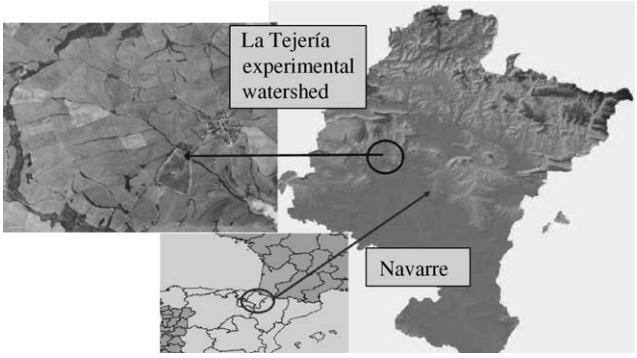

Fig. 1. Location of La Tejería experimental watershed

identified as being the most common were Tipic Xerochrepts, Fluventic Xerochrepts and Pachic Calcixerollic Xerochrepts.

The watershed covers approximately 160 ha with homogeneous slopes of around 12%, with an altitude ranging from 496 to 649 m. The watershed is almost completely cultivated and natural vegetation is only found in hedgerows and along streams. The climate is humid submediterranean, with a mean annual temperature of 13 °C. The average annual rainfall is approximately 700 mm distributed on 105 rain days.

An automated meteorological and hydrological station was established in 1994. Water quality data (sediment yield, nitrate and phosphate content and other agrochemicals) is recorded daily along with precipitation and flow discharge data taken at 10 min intervals.

During the current research period an incipient cereal crop covered most of the fields of *La Tejería* watershed, except for five fields (one ploughed field and four vegetable fields) (*Fig. 2*). The fields were classified into four classes according to their crop and tillage practise: (1) 'Cereal', conventionally sown cereal fields; (2) 'Compacted cereal', cereal fields that were compacted after sowing; (3) 'Compacted vegetables', compacted fields where vegetables were sown by scattering the seed; and (4) 'Ploughed', ploughed fields (*Figs 2* and *3*, Table 1). On each class a different number of fields was monitored in this study as detailed in Table 1.

2.2. *Satellite radar images*

RADARSAT-1 is a satellite launched by the Canadian Space Agency (CSA) in 1995 that incorporates a synthetic aperture radar (SAR) sensor operating in the C band (frequency of 5·3 GHz). RADARSAT-1 acquires images with HH polarisation, which means that

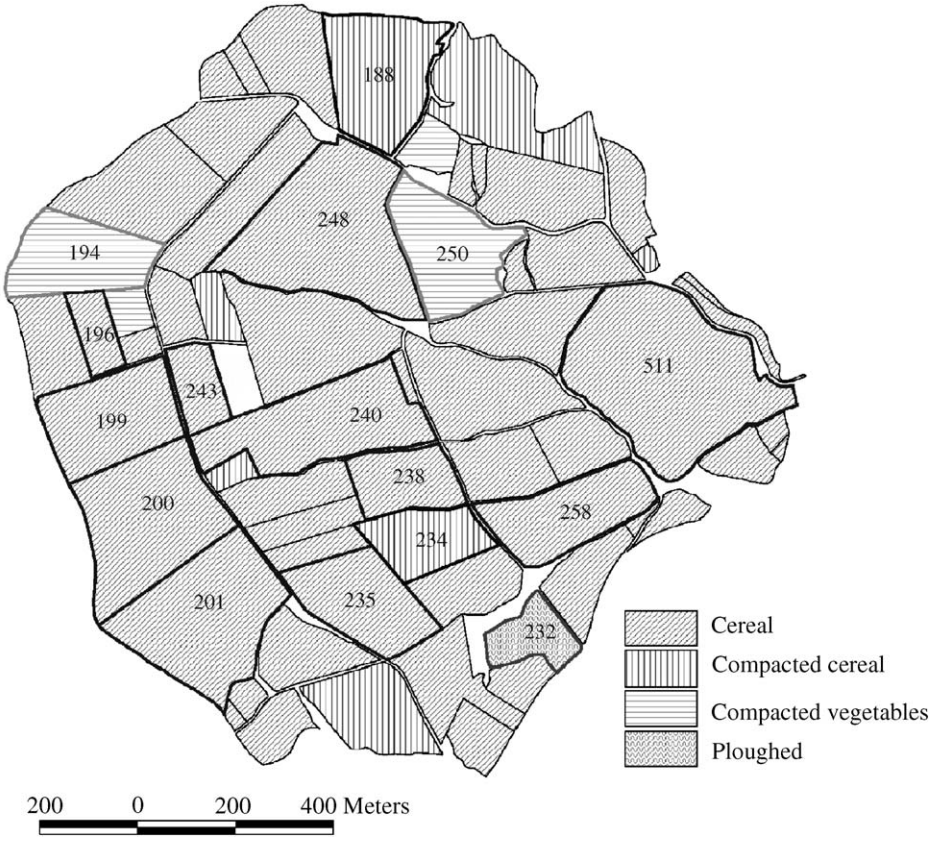

Fig. 2. Spatial distribution of observed crop classes; monitored fields appear numbered and outlined

the sensor emits and receives horizontally polarised radiation pulses.

This sensor has several operational modes that lead to different types of images according to their spatial resolution and swath width. For this study the 'Standard Mode' was adopted where images have a swath width of 100 km and a spatial resolution of about 25–30 m. In each operational mode, RADARSAT-1 is able to acquire images with different incident angles. For this research, images were selected in beam modes 1 and 2, hereafter referred as S1 and S2, respectively (where the S denotes 'Standard Mode'), that provide lower incident angles. At low incident angles vegetation-induced attenuation and surface roughness influence are minimised, yielding images more appropriate for soil moisture research (Ulaby *et al*., 1982).

RADARSAT-1 images are commercialised in a range of products depending on the required processing level. Path Image SGF (standard georeferenced fine) images, which were aligned parallel to the satellite orbital path and radiometrically corrected, were selected for this study.

The RADARSAT-1 orbital repeat cycle is of 24 days. However, combining different operation and beam modes a higher temporal coverage can be achieved.

For this research, five RADARSAT-1 SGF images were acquired over the Navarre region during spring 2003. Table 2 shows the main characteristics of the RADARSAT-1 images used in this study.

2.3. *Ground measurements*

2.3.1. *Soil moisture*

The moisture content of the soils was monitored through a stratified random sampling scheme according to the observed soil types and the considered surface state classes. Measurements were taken throughout the whole catchment on each image acquisition day, using 60 sampling points.

The soil moisture was measured using a TRIME-FM3 (IMKO, GmBH) time domain reflectometry (TDR) instrument connected to a portable three rod probe. Rods were 16 cm long, and were inserted into the soil with an angle of approximately 45° to sample the moisture content of the first 10 cm soil layer. Three TDR measurements were taken at each sampling point.

Observed moisture values reflected rainfall patterns through the research period. On the two first dates, the

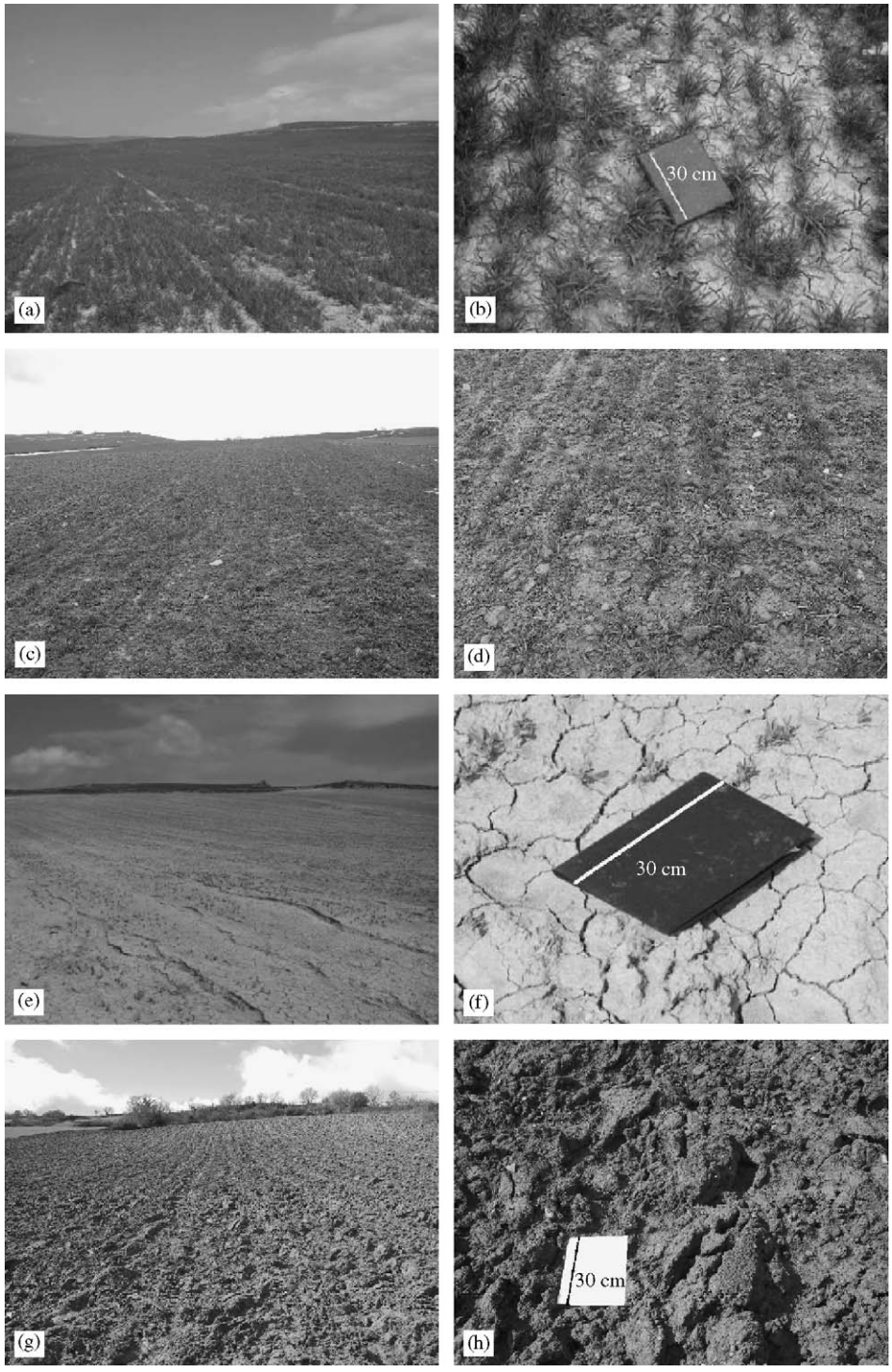

Fig. 3. Surface estate of the observed crop classes over La Tejería; 'Compacted cereal' (a, b); 'Cereal' (c, d); 'Compacted vegetables' (e, f) and 'Ploughed' (g, h)

soil moisture was high (around $0{\cdot}35\,cm^3\,cm^{-3}$). Subsequently, after 2 weeks without any precipitation, soil moisture values dropped to $0{\cdot}15$–$0{\cdot}25\,cm^3\,cm^{-3}$. For the last two dates, the moisture increased following some rainfall events (*Fig. 4*).

2.3.2. *Surface roughness*

Surface roughness was monitored collecting one-dimensional surface height profiles through a 1 m long needle profilometer with a 2 cm interval between needles.

Table 1
Description of observed crop classes; the total number of fields and area of each class is shown as well as the number of monitored fields

Class	*Description*	*No. of fields*	*Total area, ha*	*No. of monitored fields*	*Total area of monitored fields, ha*
Cereal	Winter cereal sown conventionally	52	126·27	11	59·86
Compacted cereal	Winter cereal compacted after sowing	8	17·95	2	7·90
Compacted vegetables	Chickpeas sown scattered over compacted fields	4	10·35	2	8·58
Ploughed	Ploughed fields with bare soil surface	1	1·77	1	1·77

Table 2
Main characteristics of RADARSAT-1 standard georeferenced fine (SGF) images

Date	*Time*	*Pass*	*Beam mode*	*Incident angle, deg*
27/02/2003	6:23:10	Descending	S1	20–27
06/03/2003	6:23:02	Descending	S2	24–31
23/03/2003	6:23:09	Descending	S1	20–27
30/03/2003	6:18:57	Descending	S2	24–31
02/04/2003	17:50:22	Ascending	S1	20–27

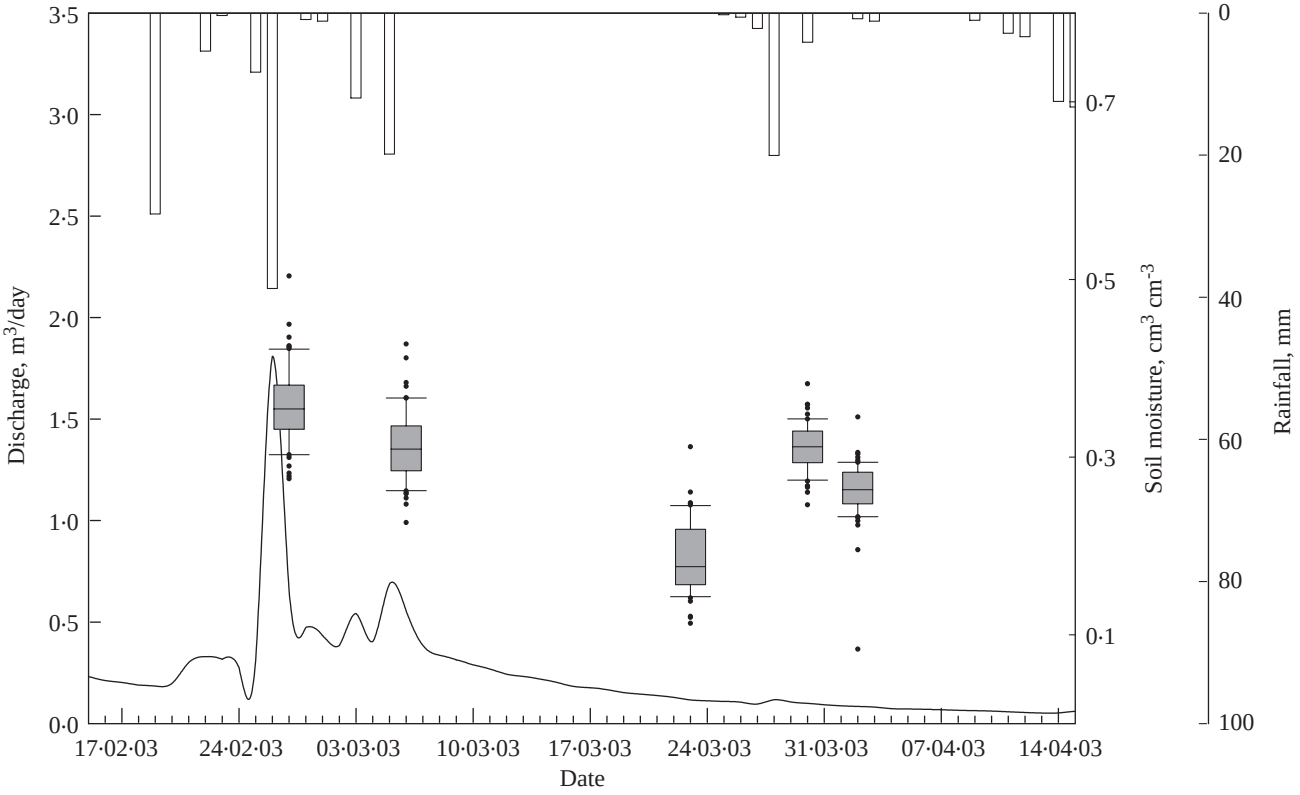

Fig. 4. Graph showing rainfall distribution, ground measured soil moisture and discharge data: □, daily accumulated rainfall; ▩, watershed soil moisture and; —, daily average discharge

Surface roughness was assumed to be homogeneous over fields belonging to each crop class (Table 1) and not variable in time because no tillage was performed during the research period. Therefore, surface roughness was sampled in order to be able to quantitatively characterise the observed four surface state classes.

Surface profiles were collected parallel to the tillage direction. Profiles were photographed, digitised, and corrected for geometrical distortions. Finally, two classical roughness parameters were derived from these profiles for each sampling point: the standard deviation of surface height s in cm and the surface correlation length l in cm. The first parameter s is a measure of the variability of the surface height (*Fig. 5*). In the case of a discrete one-dimensional soil surface profile s is calculated as follows:

$$s = \sqrt{\frac{\sum_{i=1}^{N}(z_i^2 - \bar{z}^2)}{N-1}} \quad (1)$$

where: N is the number of points in the profile; z_i is the surface height at a point i in cm; and $\bar{z}$ is the mean height of the surface profile in cm.

The surface correlation length l gives a reference for estimating the statistical independence of two points on the surface; if two points are separated by a horizontal distance larger than l, then their heights might be considered to be statistically independent of one another (Ulaby *et al.*, 1982). For its determination, the normalised autocorrelation function of the profile $\rho(x')$ must be calculated [Eqn (2)]. The surface correlation length is defined as the displacement for which the autocorrelation function is equal to 1/e (*Fig. 6*) (Ulaby *et al.*, 1982).

$$\rho(x') = \frac{\sum_{i=1}^{N+1-j} z_i z_{j+i-1}}{\sum_{i=1}^{N} z_i^2} \quad (2)$$

where: $\rho(x')$ is the autocorrelation function that measures the similarity between the height of two points separated a certain displacement $x' = (j-1)\,\Delta x$; and j is an integer $\geqslant 1$ (Ulaby *et al.*, 1982).

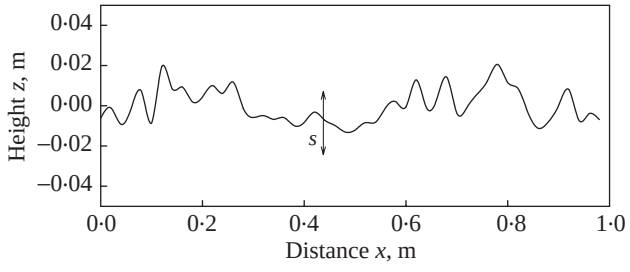

Fig. 5. Example of a surface height profile; the parameter s is the standard deviation of surface heights

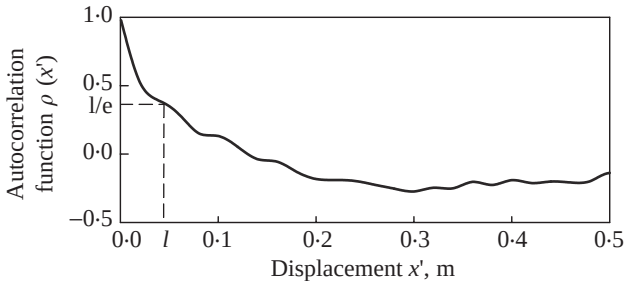

Fig. 6. Normalised autocorrelation function of a surface height profile; the correlation length l is the displacement for a correlation value that equals 1/e

The observed values for the parameter s on the different classes were: 0·467 cm for 'Compacted vegetables', 0·854 cm for 'Compacted cereal', 1·002 cm for 'Cereal', and 2·568 cm for 'Ploughed'; with standard deviations of 0·057, 0·295, 0·375 and 0·723 cm, respectively. The differentiability of the different classes was clear except for the classes 'Cereal' and 'Compacted cereal'. Data variability increased as surface became rougher (*Fig. 7*).

On the other hand, the parameter l showed the following average values for the different classes: 2·669 cm for 'Compacted vegetables', 6·082 cm for 'Compacted cereal', 5·052 cm for 'Cereal', and 7·410 cm for 'Ploughed'; with high standard deviations of 3·775, 3·780, 3·042 and 2·345 cm, respectively. The variability of this parameter was very high and seemed to increase over smooth surfaces (*Fig. 7*). The ability of parameter l to differentiate surface roughness classes is limited.

2.3.3. *Vegetation cover*

Vegetation cover data was collected in a nearby site where winter cereal was sown in the same dates with similar soil conditions and same climate. Vegetation parameters (vegetation moisture M_v, and leaf area index, I_{LA}) were measured periodically and afterwards interpolated linearly for the five image acquisition days (Table 3).

2.4. *Image processing*

Images had to be converted from 16-bit greylevels (called digital numbers) to backscattering coefficient values σ^0 in order to extract biophysical information of the terrain. This conversion was done following the standard methodology proposed by Shepherd (2000). The methodology requires information about the incidence angle of each pixel (local incidence angle). In the case of flat areas the local incidence angle can be calculated from data in the image header file. However,

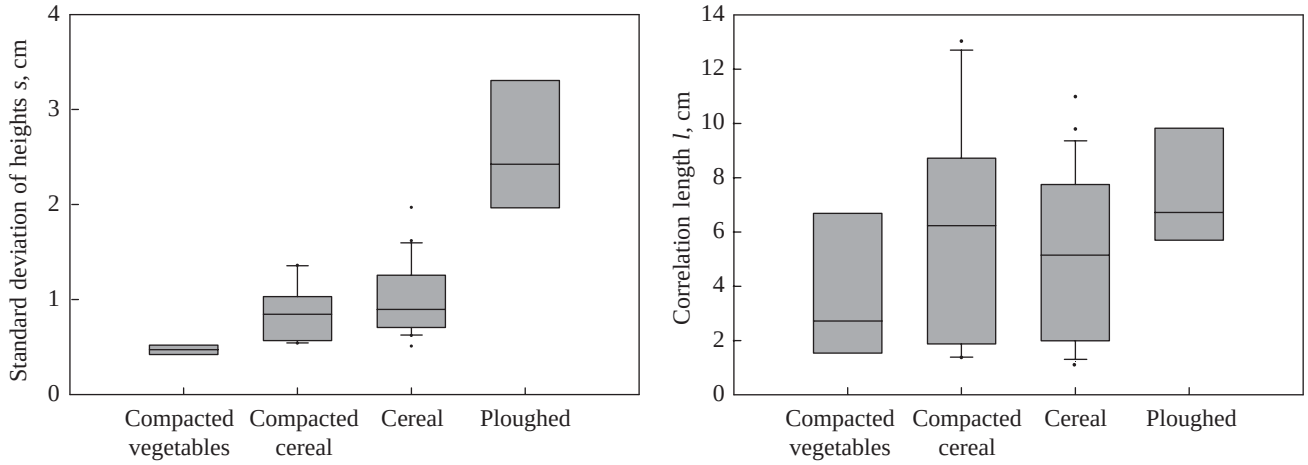

Fig. 7. Boxplots showing ground measured surface roughness parameters for each crop class; s, standard deviation of surface heights; l, surface correlation length; a high dispersion is observed specially in l values

Table 3
Estimated cereal cover parameteres for each image acquisition date

Date	*Time after sowing, days*	*Vegetation moisture (M_v), kg m^{-2}*	*Leaf area index (I_{LA})*
27/02/2003	127	0·661	2·149
06/03/2003	134	0·728	2·267
23/03/2003	151	1·056	3·048
30/03/2003	158	1·239	3·512
02/04/2003	161	1·317	3·711

Table 4
Number of ground control points collected for geocoding each image and root mean square error of the applied transformations

Image	*Number of ground control points*	*Root mean square error, pixel*
27/02/2003	5	0·81
06/03/2003	6	0·53
23/03/2003	5	0·20
30/03/2003	6	0·35
02/04/2003	5	0·91

the studied area shows a hilly topography, therefore the slope and aspect of each pixel were taken into account to calculate the local incidence angle (Ulander, 1996).

After calculating the backscattering coefficient values, the images were geocoded. Ground control points were collected and a first-order transformation was applied achieving a good coincidence between the different scenes (root mean square error values, below 1 pixel) (Table 4).

Radar images, are affected by a random interference phenomenon called speckle. Speckle causes a grainy appearance and a reduced interpretability of targets and features in the image. RADARSAT-1 SGF scenes incorporate a 4 look 'multilook' processing that reduces the magnitude of speckle by half. However, speckle was still perceptible in the scenes used, so an adaptive image filter was applied in order to reduce it over homogeneous areas. The filter selected for noise reduction was a 7 by 7 window Gamma MAP filter (Lopes *et al.*, 1990).

Finally, values of σ^0 corresponding to each ground measuring point were calculated and field and catchment average values were computed.

2.5. *Correction of the influence of vegetation*

The vegetation cover in the cereal fields consisted of incipient plants which increased in height from 10 cm, reaching 20 cm at the end of the research period. As a first approach, vegetation was assumed not to influence σ^0, and as a second approach vegetation influence was considered and corrected using a semi-empirical model.

The semi-empirical 'Water Cloud' model (Attema & Ulaby, 1978) was selected to correct for the vegetation influence. This model represents the canopy as a cloud of identical discrete scatterers that attenuate the microwave radiation and also contribute to the total canopy backscatter as shown in Eqn (3).

$$\sigma^0_{can} = \sigma^0_{veg}(\theta_{inc}) + \sigma^0_{soil}(\theta_{inc})/L^2(\theta_{inc}) \qquad (3)$$

where: $\sigma^0{}_{can}$ is the total backscattering coefficient observed from the canopy; $\sigma^0_{veg}(\theta_{inc})$ is the vegetation contribution to the total backscattering depending on the incident angle; $\sigma^0_{soil}(\theta_{inc})$ is the contribution of the

soil that is attenuated twice by the canopy through its loss factor $L(\theta_{inc})$.

As the low degree of development of the canopy $\sigma^0_{veg}(\theta_{inc})$ can be considered negligible, assuming that the canopy only acts attenuating the radiation (Taconet *et al.*, 1996), the vegetation loss factor depends on vegetation cover water content (M_V in kg m^{-2}) and incident angle as shown in Eqn (4) (Ulaby *et al.*, 1982):

$$L(\theta_{inc}) = \exp(B_1 M_V / \cos\theta_{inc}) \quad (4)$$

where: B_1 is an empirical constant.

Shifting to dB units of measurement and assuming that, for a given soil roughness, $\sigma^0_{soil,\mathrm{dB}}(\theta_{inc})$ depends linearly on the soil moisture M_S in %, as shown in Eqn (5), Eqn (6) is obtained

$$\sigma^0_{soil,dB}(\theta_{inc}) = CM_S + D \quad (5)$$

$$\sigma^0_{can,dB} = \frac{-20B_1}{\ln 10 \cos\theta_{inc}} M_V + CM_S + D \quad (6)$$

where: B_1, C and D are empirical constants that can be easily obtained through multiple regression or least square techniques once M_S and M_V are known.

Therefore, soil surface backscattering values for $\sigma^0_{soil,\mathrm{dB}}(\theta_{inc})$ can be obtained by subtracting the vegetation attenuation term from the RADARSAT-1 sensed backscattering values $\sigma^0_{can,\mathrm{dB}}$:

$$\sigma^0_{soil,dB}(\theta_{inc}) = \sigma^0_{can,dB} - \left(\frac{-20B_1}{\ln 10 \cos\theta_{inc}} M_V\right) \quad (7)$$

3. Results and discussion

In the present research, surface roughness was assumed to be constant in time. Under this assumption, it is possible to consider that, for each class, σ^0 is linearly related to the soil moisture (Ulaby *et al.*, 1982) and associate σ^0 variations to moisture variations. In this section, the correlation between σ^0 and the soil moisture is analysed at three scales: point scale, field scale and catchment scale. The influence of the vegetation is assessed and, finally, the ability of the RADARSAT-1 images to discriminate soil moisture classes is studied.

3.1. *Point scale correlation*

Ground measured soil moisture values were compared to σ^0 values at pixel level through the five different image acquisition days. According to the assumption of homogeneous surface conditions (surface roughness and vegetation cover, for each considered class); a unique regression line was fitted for all the points belonging to the same class (*Fig. 8*). These regressions showed low correlation values: a direct relation was observed between both variables but dispersion was high in all classes. This variability can be due to several causes. Firstly, the influence of speckle causes pixel values to vary randomly even after filtering the images; secondly, discrete soil moisture point measurements were compared to σ^0 values corresponding to one pixel (approximately 12·5 m by 12·5 m). Finally, the variability of the surface roughness parameters on each class can also cause the correlation coefficient to decrease.

3.2. *Field scale correlation*

Comparing the soil moisture measurements with the σ^0 values at the field scale would a priori yield better results because some of the variability observed at the point scale could be reduced. For individual fields, both variables showed good agreement in most cases (Table 5). Fields belonging to the classes 'Cereal', 'Compacted cereal' and 'Compacted Vegetables' showed high correlation values. Slope values ranged from 1·210 to 2·679 in the class 'Cereal' and were higher in the smoother classes 'Compacted cereal' and 'Compacted vegetables' (2·823–3·287 and 4·057–5·900, respectively). Intercept values ranged from 38·001 to 46·858 in the class 'Cereal'; 51·916 and 54·693 in 'Compacted cereal'; and 57·711 and 74·935 in 'Compacted vegetables'. The ploughed field had the lower correlation value.

Assuming identical surface conditions in fields belonging to the same class, a unique trend line was fitted for each class (*Fig. 9*). This time, agreement was good in classes 'Compacted cereal' and 'Compacted Vegetables', albeit the low number of fields considered (only two per class) might be insufficient to extract any solid conclusions. The class 'Cereal' showed a high data variability meaning that fields cannot be considered as homogeneous. These differences between 'Cereal' fields can also be noticed in the variability of slope values for each independent field (Table 5).

In the case of 'Cereal' and 'Compacted cereal' fields the vegetation cover could influence σ^0. The previously mentioned 'Water Cloud' model was applied to account for the vegetation attenuation. Apparently, the model described adequately the influence of the vegetation (Table 6). In the case of 'Cereal' fields the improvement was clear, from a value of the coefficient of determination R^2 of 0·444 (*Fig. 9*) to R^2 of 0·675 (Table 6); whereas in the 'Compacted cereal' fields the improvement was slight, from a value for R^2 of 0·815 (*Fig. 9*) to R^2 of 0·827 (Table 6).

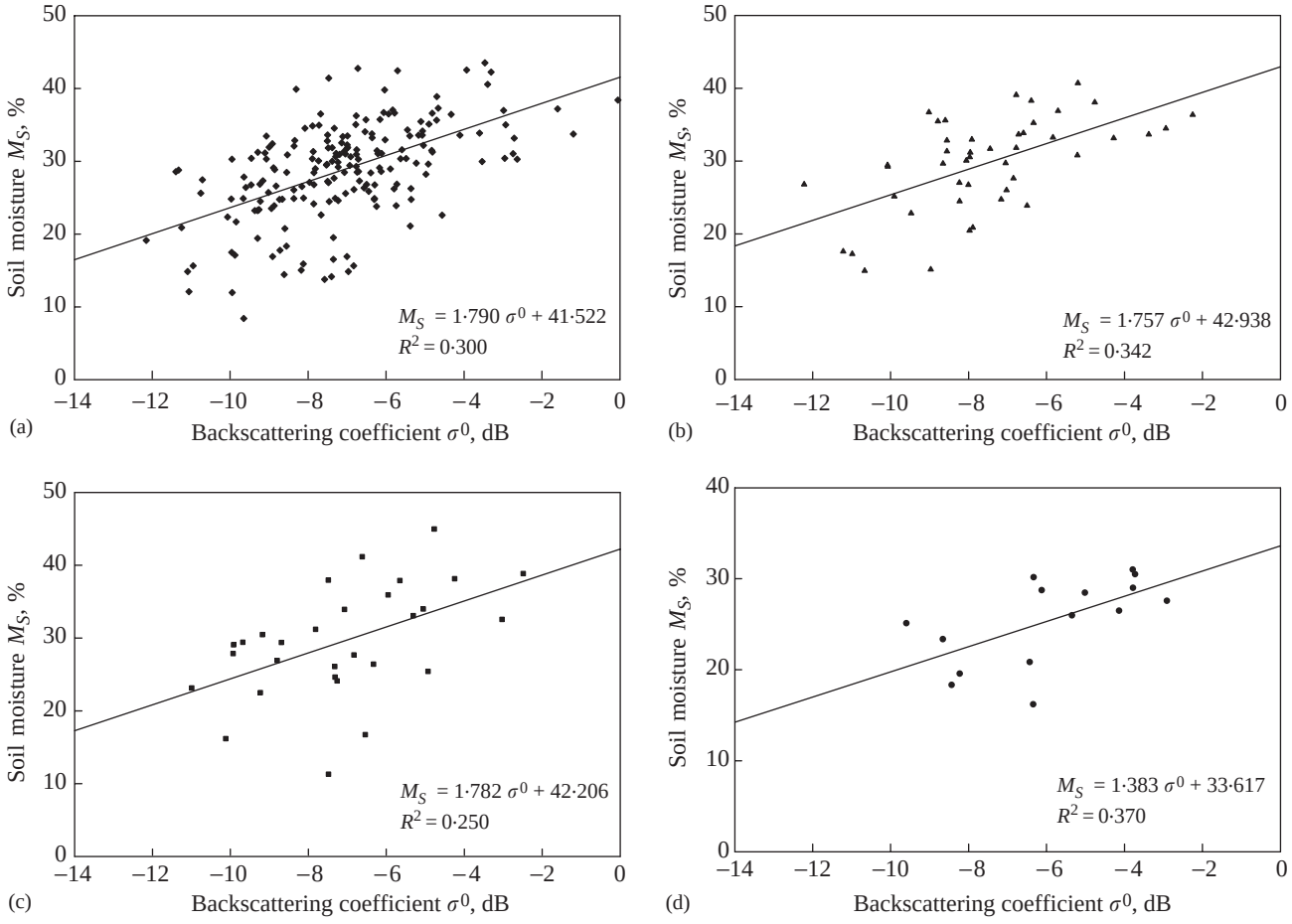

Fig. 8. Linear regression models between ground measured soil moisture (M_S) and the backscattering coefficient σ^0 at the point scale for points belonging to each class: (a) 'Cereal'; (b) 'Compacted cereal'; (c) 'Compacted vegetables'; (d) 'Ploughed'; R^2, coefficient of determination

3.3. *Catchment scale correlation*

The next spatial aggregation level studied was the catchment scale. The experimental catchment used in this study is small (160 ha), and therefore this spatial scale can still be considered relevant for hydrological and agronomic applications. Catchment average soil moisture and σ^0 values were compared using data corresponding to the five acquired scenes. Observed agreement was good (*Fig. 10*). At this scale, variability caused by surface roughness variability, vegetation cover and other surface characteristics seems to decrease being σ^0 more sensible to the soil moisture variations (Cognard *et al.*, 1995; van Oevelen *et al.*, 1996). At high aggregation levels the influence of speckle also decreases.

The observed linear regression shows a good correlation, and the obtained slope and intercept were close to values obtained by other authors (Le Hegarat-Mascle *et al.*, 2002). Although correlation was good, vegetation cover could be attenuating σ^0 values as observed at the field scale. The 'Water Cloud' model was also applied at the catchment scale leading to Eqn (8) and achieving a value for R^2 of 0·926:

$$\sigma^0_{can} = \frac{-1{\cdot}364 M_V}{\cos\theta_{inc}} - 10{\cdot}329 + 0{\cdot}161 M_S \qquad (8)$$

3.4. *Discrimination of soil moisture classes*

The ability of the proposed linear relations for discriminating different soil moisture ranges or classes was tested. Three different soil moisture classes were identified according to crop development issues.

(a) Class 1—low soil moisture values < 20%

At low soil moisture values, plants are unable to extract a sufficient amount of water from the soil. Crops

Table 5
Observed linear regression models for each field

Class	*Field no.*	*Slope*	*Intercept*	R^2
Cereal	196	1·418	38·309	0·736
	199	1·210	38·252	0·834
	200	1·960	38·001	0·499
	201	2·028	40·718	0·709
	235	1·750	41·586	0·808
	238	2·341	44·837	0·807
	240	1·366	39·434	0·810
	243	2·679	43·906	0·664
	248	2·639	46·858	0·826
	258	1·776	41·134	0·737
	511	1·620	44·102	0·798
Compacted cereal	188	3·287	54·693	0·793
	234	2·823	51·916	0·833
Compacted vegetables	194	4·057	57·711	0·648
	250	5·900	74·935	0·938
Ploughed	232	1·492	34·281	0·483

Fields are grouped into classes and the slope, intercept and coefficient of determination R^2 are given for each linear regression model.

can experience severe yield reductions depending on the magnitude of the water deficit and its duration.

(b) Class 2–medium soil moisture values of 20–30%

These moisture conditions are assumed to allow crop growth and development in optimal conditions.

(c) Class 3—high soil moisture values > 30%

Excessive soil moisture values also cause yield reductions by hampering the root respiration rate. On the other hand, the occurrence of pests, such as fungal

Table 6
Fitted 'Water Cloud' model equations for 'Cereal' and 'Compacted cereal' fields, which values for the different of determination R^2

Class	*Model coefficients*			R^2
	B_1	C	D	
Cereal	0·244	0·157	−9·144	0·675
Compacted cereal	0·084	0·247	−14·270	0·827

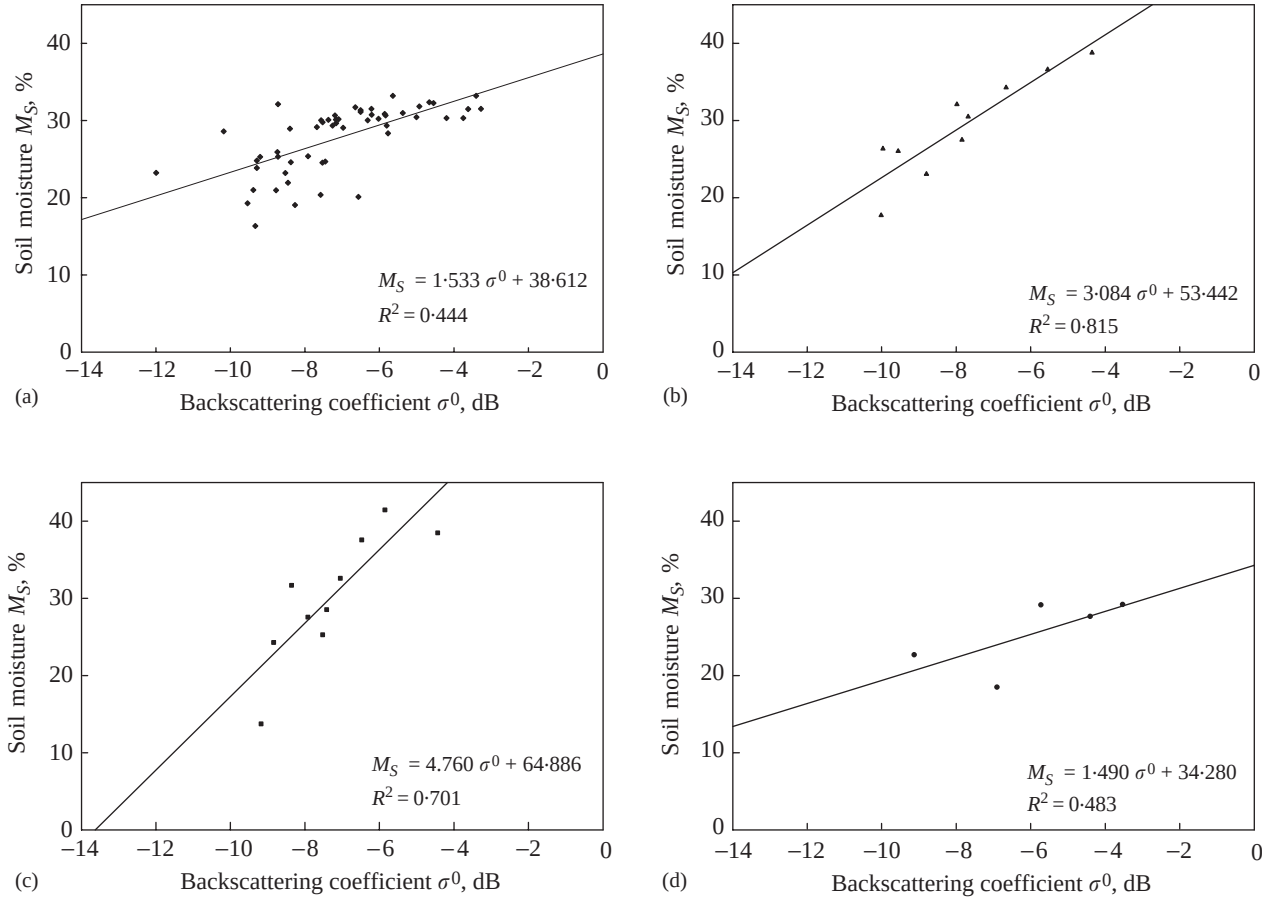

Fig. 9. Linear regression models between ground measured soil moisture (M_S) and the backscattering coefficient σ^0 at the field scale for fields belonging to each class: (a) 'Cereal'; (b) 'Compacted cereal';(c) 'Compacted vegetables';(d) 'Ploughed'; R^2, coefficient of determination

infestations, is favoured affecting crop development as well.

The ability of RADARSAT-1 derived σ^0 for discriminating between moisture classes was assessed at the field and catchment scale. A clear differentiation between classes will provide a means for detecting whether crops are suffering any kind of moisture related stress. The analysis of the variance (ANOVA) test was used to see if there was any significant difference in σ^0 for the considered moisture classes.

On the other hand, the influence of vegetation attenuation was also evaluated by looking at the discrimination ability of corrected backscattering values [Eqn (7)].

At the field scale the ANOVA test indicated that there were statistically significant differences on the backscattering coefficient of the three considered moisture classes. However, the three classes showed a certain overlap that was particularly noteworthy between classes 1 and 2 (Table 7).

Although the separation between Classes 1 and 2 was not clear, σ^0 values above $-6{\cdot}416$ dB could be considered to belong to Class 3 with a 95% confidence (Table 7).

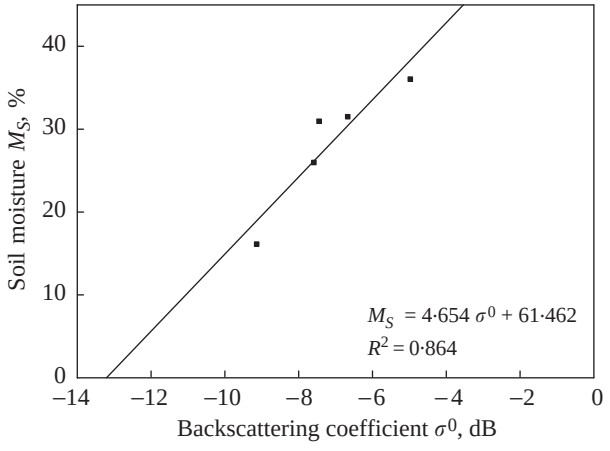

Fig. 10. Linear regression model between the backscattering coefficient σ^0 and ground measured soil moisture (M_S) at the catchment scale; R^2, coefficient of determination

At the catchment scale, the separation between the three classes was more evident [*Fig. 11(a)*]. However, the number of data available ($N = 5$) limited the analysis. Approximately, σ^0 values below $-8{\cdot}0$ dB could be assigned to Class 1 and values above $-6{\cdot}5$ dB to Class 3, while Class 2 ranged between those two values. These class limits are consistent with those observed at the field scale (Table 7), however more observations would be needed to draw more consistent conclusions.

After correcting the σ^0 values for the vegetation attenuation, the results were quite similar although class limit increased in value (Table 8). The ANOVA test found significant differences between the three classes at the field scale, as well as at the catchment scale. At the field scale, despite the existing overlap between classes, the estimated intervals for each class at the 95% confidence level were clearer than before correcting for the vegetation attenuation (Table 8).

Values of σ^0 below -7 dB could be classified as Class 1 and values of σ^0 above -5 dB to Class 3. Class 2 seemed to have quite a reduced variation range, approximately from -7 to -5 dB. At the catchment scale, although proposed classification seemed to be reasonable [*Fig. 11(b)*], more observations are needed to obtain statistically significant class limits.

4. Conclusions

The use of linear regression models in determining the relationship between the RADARSAT-1 backscattering coefficient σ^0 and the top soil moisture content M_S was investigated. Such relationship makes the retrieval of soil moisture from backscattered values simple as it does not require the measurement of other surface characteristics, such as soil roughness.

Fitted linear regressions between σ^0 and the soil moisture showed that correlation values improve from pixel scale to field scale and further up to catchment scale. This indicates that at high aggregation levels the variability of surface characteristics, such as roughness, is averaged and therefore σ^0 becomes more sensitive to soil moisture variations.

Table 7
Statistical description of σ^0 values belonging to each class at the field scale; the number of fields (N) is given along with the mean, standard deviation and typical error of σ^0, and its expected interval at 95% confidence

	N	*Mean σ^0, dB*	*Standard deviation σ^0, dB*	*Typical error, dB*	*95% Confidence interval for the mean σ^0, dB*	
					Lower limit	*Upper limit*
Class 1	6	−8·873	1·120	0·457	−10·048	−7·698
Class 2	41	−8·094	1·617	0·252	−8·604	−7·583
Class 3	37	−5·948	1·404	0·231	−6·416	−5·480

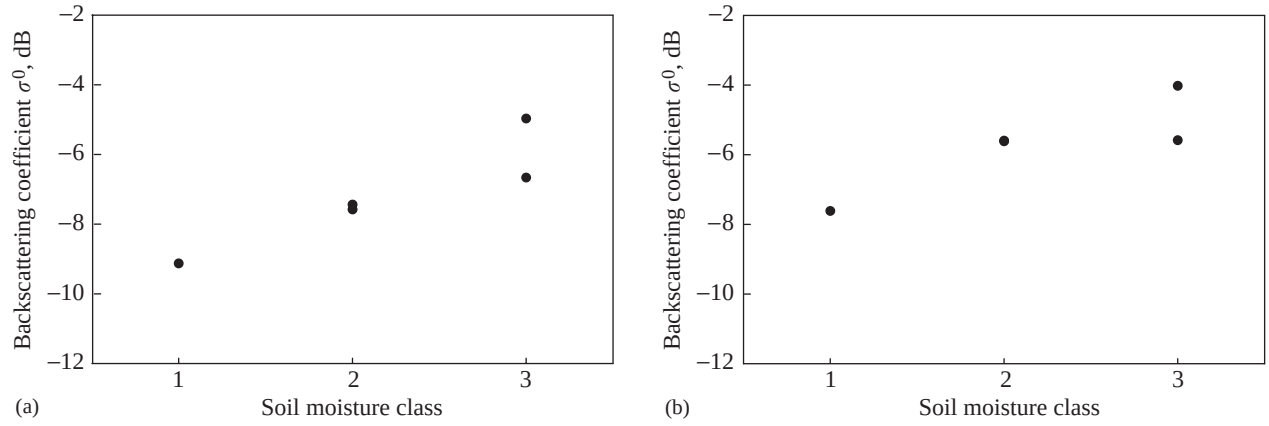

Fig. 11. Scatterplot of backscattering values for each soil moisture class at the catchment scale; Class 1 corresponds to soil moisture values below 20%, Class 2 ranges from 20% to 30% and Class 3 represents moisture values above 30%. (a) Backscattering values with no correction for the vegetation attenuation, and (b) corrected backscattering values

Table 8
Statistical description of σ^0 values belonging to each class at the field scale after correcting the vegetation attenuation on σ^0 values the number of fields (*N*) is given along with the mean, standard deviation and typical error of σ^0, and its expected interval at 95% confidence

	N	*Mean σ^0, dB*	*Standard deviation σ^0, dB*	*Typical error, dB*	*95% Confidence interval for the mean σ^0, dB*	
					Lower limit	*Upper limit*
Class 1	6	−7·574	1·318	0·538	−8·958	−6·190
Class 2	41	−6·370	1·921	0·300	−6·976	−5·763
Class 3	37	−4·516	1·585	0·260	−5·045	−3·988

Crops and vegetation covers, also influence σ^0, hampering the retrieval of soil moisture over vegetated areas. In the case of incipient cereal crops, the vegetation cover can be assumed only to attenuate the backscattered signal from the soil surface. This attenuation can be calculated as a function of the vegetation moisture content by means of the semi-empirical 'Water Cloud' model, providing a straightforward means for correcting the σ^0 values.

In this study, it has been found that RADARSAT-1 derived σ^0 values can be used to discriminate soil moisture classes. After correcting the vegetation attenuation, fields with values of σ^0 below -7 dB can be classified as Class 1 (moisture values below 20%) with a 95% confidence level, and therefore, can be considered to experience some degree of water stress. In the same manner, fields with values of σ^0 above -5 dB can be classified as Class 3 (moisture values above 30%) with a 95% confidence level, and will be prone to suffer some kind of stress related to an excessive water content of the soil, such as fungal infestations.

At the catchment scale, the variability within classes seemed to decrease, thus indicating that the classification in moisture classes could be more accurate for large fields or higher aggregation levels.

The presented approach is completely empirical and needs to be validated in following campaigns, especially over moisture conditions higher and lower than the conditions of the present study. The consistency of the linear regressions and the class limits will also be tested to evaluate the application of this technique on an operational manner.

On the other hand, the approach is simple to apply as surface roughness ground measurements are not needed for its application. It will be useful for application scenarios such as crop growth monitoring and modelling, where an approximate knowledge of the moisture content of soils is required but very detailed soil moisture estimations are not needed.

The fact that at coarser spatial scales the accuracy of the soil moisture retrieval improved is relevant for hydrological applications, because runoff predictions

can be improved if the average soil moisture content of the catchment before a rainfall event is known.

Acknowledgements

The authors would like to thank the Canadian Space Agency for granting 5 RADARSAT-1 SGF scenes under the *Data for Research Use* program project No. DRU-10-02. This work was part of a project financed by the Spanish Government's National Scientific Research, Development and Technological Innovation Plan, project code REN2003-03028/HID. The work was also part of the Agreement No. 58-6408-0-F137 with the US Department of Agriculture. Any opinions, findings, conclusion, or recommendations expressed in this publication are those of the authors and do not necessarily reflect the view of the US Department of Agriculture.

References

Altese E; Bolognani O; Mancini M; Troch P A (1996). Retrieving soil moisture over bare soil from ERS-1 synthetic aperture radar data: sensitivity analysis based on a theoretical surface scattering model and field data. Water Resources Research, **32**(3), 653–661

Attema E W P; Ulaby F T (1978). Vegetation modelled as a water cloud. Radio Science, **13**(2), 357–364

Burman R D (2003). Evapotranspiration formulas. In: Encyclopaedia of Water Science (Stewar B A; Howell T A, eds), pp 253–257. Marcel Dekker, USA

Casalí J; López J J; Giráldez J V (1999). Ephemeral gully erosion in southern Navarra, Spain. Catena, **36,** 65–84

Cognard A L; Loumagne C; Normand M; Olivier P; Ottlé C; Vidal-Madjar D; Louahala S; Vidal A (1995). Evaluation of the ERS 1/synthetic aperture radar capacity to estimate surface soil moisture: two-year results over the Naizin watershed. Water Resources Research, **31**(4), 975–982

Chanzy A (2003). Evaporation from soils. In: Encyclopaedia of Water Science (Stewar B A; Howell T A, eds), pp 249–251. Marcel Dekker, USA

Davidson M W J; Le Toan T; Mattia F; Satalino G; Manninen T; Borgeaud M (2000). On the characterisation of agricultural soil roughness for radar remote sensing studies. IEEE Transactions on Geoscience and Remote Sensing, **38**(2), 630–640

Donézar M; del Valle de Lersundi J (2001). The experimental watershed network in Navarre. XIX Spanish National Congress of Irrigation, Zaragoza, Spain (In Spanish)

Famiglietti J S; Devereaux J A; Laymon C A; Tsegaye T; Houser P R; Jackson T J; Graham S T; Rodell M; van Oevelen P J (1999). Ground based investigation of soil moisture variability within remote sensing footprints during the SGP 97 hydrology experiment. Water Resources Research, **35**(6), 1839–1851

Fung A K (1994). Microwave Scattering and Emission Models and their Applications. Artech House, Nordwood, USA

Georgakakos K P; Baumer O W (1996). Measurement and utilisation of on-site soil moisture data. Journal of Hydrology, **184,** 131–152

Government of Navarre (2000). Soil map of *La Tejería* (Villanueva de Yerri) experimental watershed. Internal Report made by the Soils and Climate Section of the Agricultural Structure Service, Department of Agriculture, Farming and Food, Government of Navarre, Pamplona, Spain (In Spanish)

Huisman J A; Snepvangers J; Bouten W; Heuvelink G B (2002). Mapping spatial variation in surface soil water content: comparison of ground-penetrating radar and time domain reflectometry. Journal of Hydrology, **269,** 194–207

Jackson T J (1980). Profile soil moisture from surface measurements. Journal of Irrigation and Drainage Division Proceedings, **106,** 81–92

Kachanoski R G; Gregorich E G; van Wesenbeeck I J (1988). Estimating spatial variations of soil water content using noncontacting electromagnetic inductive methods. Canadian Journal of Soil Science, **68,** 715–722

Kirkby M J (2001). Modelling the interactions between soil surface properties and water erosion. Catena, **46,** 89–102

Le Hegarat-Mascle S; Zribi M; Alem F; Weisse A; Loumagne C (2002). Soil moisture estimation from ERS/SAR data: Toward an operational methodology. IEEE Transactions on Geoscience and Remote Sensing, **40**(12), 2647–2658

Lopes A; Touzi R; Nezry E (1990). Adaptive speckle filters and scene heterogeneity. IEEE Transactions on Geoscience and Remote Sensing, **28**(6), 992–1000

Mancini M; Hoeben R; Troch P A (1999). Multifrequency radar observations of bare soil surface soil moisture content. A laboratory experiment. Water Resources Research, **35**(6), 1827–1838

Montgomery D R; Dietrich W E (1988). Where do channels begin?. Nature, **336,** 232–234

Moore I D; Burch G J; Mackenzie D H (1988). Topographic effects on the distribution of surface soil water and the location of ephemeral gullies. Transactions of the ASAE, **31,** 1098–1107

Moran M S; Perts-Lidard C D; Watts J M; McElroy S (2004). Estimating soil moisture at the watershed scale with satellite-based radar and land surface models. Canadian Journal of Remote Sensing, **30**(5), 805–826

Oh Y; Sarabandi K; Ulaby F T (1992). An empirical model and an inversion technique for radar scattering from bare soil surfaces. IEEE Transactions on Geoscience and Remote Sensing, **30**(2), 370–381

O'Loughlin E M (1986). Prediction of surface saturation zones in natural catchments by topographic analysis. Water Resources Research, **22**(5), 794–804

Quesney A; Le Hégarat-Mascle S; Taconet O; Vidal-Madjar D; Wigneron J P; Loumagne C; Normand M (2000). Estimation of watershed soil moisture index from ERS/SAR data. Remote Sensing of Environment, **72**(3), 290–303

Rodríguez-Iturbe I (2000). Ecohydrology: a hydrologic perspective of climate–soil–vegetation dynamics. Water Resources Research, **36,** 3–9

Romkens M J M; Helming K; Prasad S N (2001). Soil erosion under different rainfall intensities, surface roughness and soil water regimes. Catena, **46,** 103–123

Rowntree P R; Bolton J A (1983). Simulation of the atmospheric response to soil moisture anomalies over Europe. Quarterly Journal of the Royal Meteorological Society, **109,** 501–526

Shepherd N (2000). Extraction of beta nought and sigma nought from RADARSAT CDPF products. (Tech. Rep. Altrix. systems), Ottawa, Canada

Taconet O; Vidal-Madjar D; Emblanch Ch; Normand M (1996). Taking into account vegetation effects to estimate soil moisture from C-band radar measurements. Remote Sensing of Environment, **56,** 52–56

Troch P A; Mancini M; Paniconi C; Wood E F (1993). Evaluation of a distributed catchment scale water balance model. Water Resources Research, **29**(6), 1805–1817

Troch P A; Paniconi C; McLaughlin D (2003). Catchment-scale hydrological modeling and data assimilation. Advances in Water Resources, **26**(2), 131–135

Ulaby F T; Moore R K; Fung A K (1982). Microwave Remote Sensing, Active and Passive, Vol. II: Radar Remote Sensing and Surface Scattering and Emission Theory. Artech House, Nordwood, USA

Ulander L (1996). Radiometric slope correction of synthetic aperture radar images. IEEE Transactions on Geoscience and Remote Sensing, **34**(5), 1115–1122

van Oevelen P J; Hoekman D H; Feddes R A (1996). Errors in estimation of areal soil water content from SAR data. In: Scaling Up in Hydrology Using Remote Sensing (Stewart J B, ed), pp 207–220. Wiley, Chichester, UK

Wetzel P J; Chang J T (1987). Concerning the relationship between evapotranspiration and soil moisture. Journal of Climate and Applied Meteorology, **26,** 18–27

Yu Z; Carlson T N; Barron E J; Schwartz F W (2001). On evaluating the spatial temporal variation of soil moisture in the Susquehanna river basin. Water Resources Research, **37**(5), 1313–1326